



This is a repository copy of *Static assessment of notched additively manufactured acrylonitrile butadiene styrene (ABS)*.

White Rose Research Online URL for this paper:  
<http://eprints.whiterose.ac.uk/169082/>

Version: Published Version

---

**Proceedings Paper:**

Ng, C.T. and Susmel, L. [orcid.org/0000-0001-7753-9176](https://orcid.org/0000-0001-7753-9176) (2020) Static assessment of notched additively manufactured acrylonitrile butadiene styrene (ABS). In: Iacoviello, F., Sedmak, A., Marsavina, L., Blackman, B., Ferro, G.A., Shlyannikov, V., Ståhle, P., Zhang, Z., Moreira, P.M.G.P., Božic, Ž. and Banks-Sills, L., (eds.) *Procedia Structural Integrity*. 1st Virtual European Conference on Fracture - VECF1, 29 Jun - 01 Jul 2020, Virtual conference. Elsevier , pp. 627-636.

<https://doi.org/10.1016/j.prostr.2020.10.073>

---

**Reuse**

This article is distributed under the terms of the Creative Commons Attribution-NonCommercial-NoDerivs (CC BY-NC-ND) licence. This licence only allows you to download this work and share it with others as long as you credit the authors, but you can't change the article in any way or use it commercially. More information and the full terms of the licence here: <https://creativecommons.org/licenses/>

**Takedown**

If you consider content in White Rose Research Online to be in breach of UK law, please notify us by emailing [eprints@whiterose.ac.uk](mailto:eprints@whiterose.ac.uk) including the URL of the record and the reason for the withdrawal request.



[eprints@whiterose.ac.uk](mailto:eprints@whiterose.ac.uk)  
<https://eprints.whiterose.ac.uk/>



1st Virtual European Conference on Fracture

# Static assessment of notched additively manufactured acrylonitrile butadiene styrene (ABS)

Chin Tze Ng, Luca Susmel\*

*Department of Civil and Structural Engineering, The University of Sheffield, Mappin Street, Sheffield, S1 3JD, United Kingdom*

---

## Abstract

The present paper tackles the problem of performing the static assessment of notched additively manufactured (AM) acrylonitrile butadiene styrene (ABS) components. A large number of ABS specimens containing different notch profiles and sharpness were manufactured (flat on build plate) by varying the printing angles to simulate the stress concentration phenomena. These specimens were tested under tension and three-point bending to generate a large amount of experimental data. From the experimental results, it is evident that the AM ABS materials can simply be modelled as an elastic, brittle, homogenous and isotropic material. This simplification allowed the application of the Theory of Critical Distances (TCD) to become a viable static assessment tool for the AM ABS components. As a result, it was proven that the TCD is an accurate and valid static assessment tool for the AM ABS components with estimations mainly falling within an error interval of about  $\pm 20\%$ . This result is certainly rewarding from an engineering application perspective as the TCD successfully enables engineers to assess the static strength of additively manufactured engineering components that contain intricate geometrical features accurately, rapidly, and economically.

© 2020 The Authors. Published by Elsevier B.V.

This is an open access article under the CC BY-NC-ND license (<https://creativecommons.org/licenses/by-nc-nd/4.0>)

Peer-review under responsibility of the European Structural Integrity Society (ESIS) ExCo

*Keywords:* Additive manufacturing; Acrylonitrile Butadiene Styrene (ABS); Notch; Critical Distance

---

---

\* Corresponding author.

*E-mail address:* [lsusmel@sheffield.ac.uk](mailto:lsusmel@sheffield.ac.uk)

## 1. Introduction

Due to the advancement of technology, additive manufacturing (AM) is currently capable of rapidly manufacturing objects at a relatively lower cost. This clearly suggests that AM has a tremendous potential in underpinning the revolution of the manufacturing industry. Thus, one could expect the existence of structures with intricate geometries to be more common in the near future. However, this is of concern from a structural integrity perspective as localised stress concentration is an inevitable side effect for structures containing complex geometrical features. In this scenario, it is essential for engineers to accurately perform static assessment of AM components containing various geometrical features. Hence, reliable and simplistic theoretical tools that can predict the static strength of AM engineering components become invaluable to practitioners.

### Nomenclature

|                                       |   |
|---------------------------------------|---|
| E                                     | Young's modulus   |
| a, B, W                               | dimensions of the C(T) specimens according to ASTM D5045–14 |
| $F_f$                                 | failure force   |
| $K_c$                                 | fracture toughness  |
| $K_{IC}$                              | plane strain fracture toughness                             |
| L                                     | critical distance   |
| O $\theta$ r                          | polar coordinates   |
| Oxy                                   | local system of coordinates                                 |
| $P_{max}$ , $P_Q$                     | forces determined according to ASTM D5045-14                |
| R                                     | notch root radius   |
| $S_D$                                 | standard deviation  |
| t                                     | specimen's thickness  |
| $w_n$ , $w_g$                         | net and gross width   |
| $\theta_p$                            | manufacturing angle   |
| $\sigma_{0.1\%}$                      | 0.1% proof stress   |
| $\sigma_1$                            | maximum principal stress                                    |
| $\sigma_{eff}$                        | effective stress  |
| $\sigma_{UTS}$                        | ultimate tensile strength                                   |
| $\sigma_x$ , $\sigma_y$ , $\tau_{xy}$ | local stress components                                     |
| $\sigma_Y$                            | yield stress  |
| $\alpha$                              | notch opening angle   |

In this context, attention will be focused on the additively manufactured acrylonitrile butadiene styrene (ABS) –  $(C_8H_8C_4H_6C_3H_3N)_n$  thermoplastic polymer. Due to its high impact and resistance to corrosion, ABS as an engineering polymer is commonly used to produce rigid and lightweight engineering components. In light of recent technological developments, ABS has become one of the popular polymers that can be rapidly additively manufactured by making use of the Fused Filament Fabrication (FFF) technique.

To fully exploit the use of AM ABS in practical engineering applications, it is essential to find an accurate and robust static assessment tool that can take stress concentration effects into account. Therefore, the present paper aims to bridge the knowledge gap of stress concentration effects on AM engineering components by validating the accuracy and robustness of the Theory of Critical Distances (TCD) as an effective static assessment tool.

## 2. Experimental details

Plain, notched, and compact tension (C(T)) specimens with configurations as shown in Fig.1 were manufactured by the FFF-based Ultimaker 2 Extended+ 3D-printer using grey filaments of PRIMA 750g ABS with diameter of 2.85 mm (Ng and Susmel, 2020). The constant manufacturing parameters for all specimens were set as follows:

extrusion nozzle diameter equal to 0.4mm, nozzle temperature kept at 255°C, build plate temperature to 90°C, printing rate of 30mm/s, infill density equal to 100%, height of layers to 0.1mm, and shell thickness set to 0.4mm (Ng and Susmel, 2020).

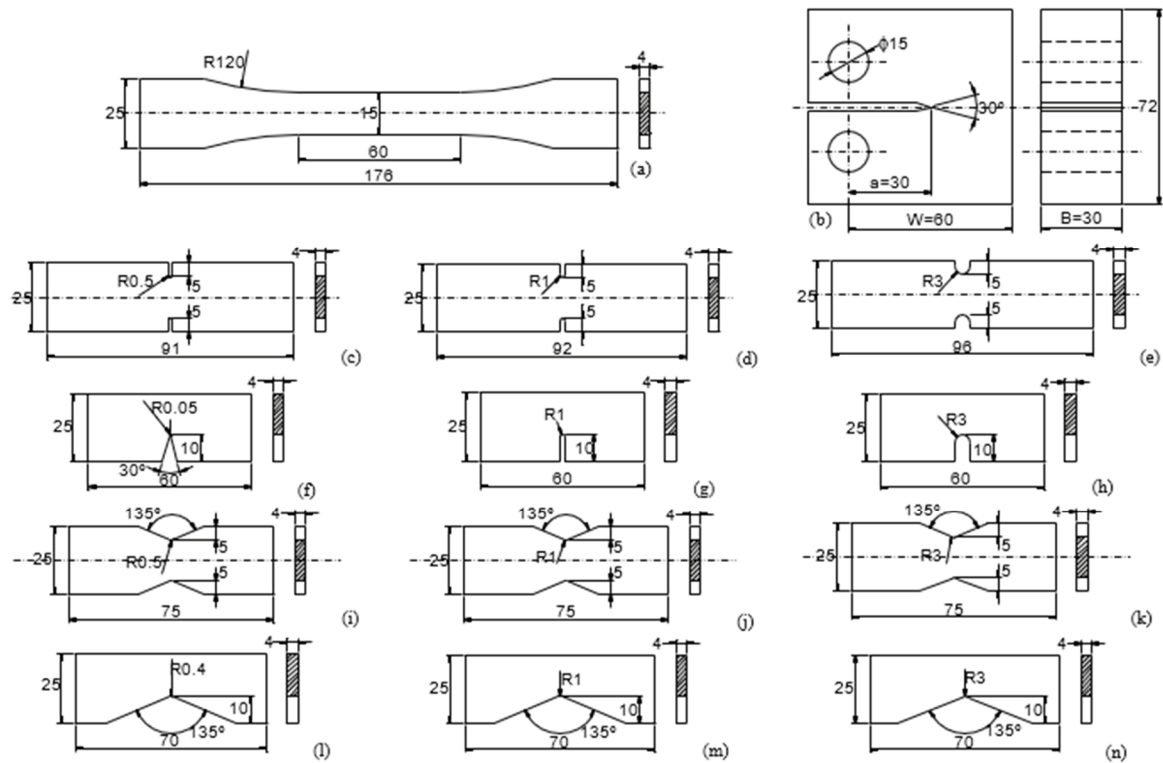


Fig. 1. Configurations of investigated specimens (dimensions in millimeters).

Notably, all specimens were manufactured flat on the build plate as depicted in Fig. 2 (Ng and Susmel, 2020). In order to investigate the effects of different material lay-ups on the mechanical properties of the AM ABS specimens, the manufacturing angle,  $\theta_p$  is varied in the range of 0° to 90°. The relationship between manufacturing angle,  $\theta_p$  and its corresponding material lay-up is illustrated in Fig. 3 (Ng and Susmel, 2020).

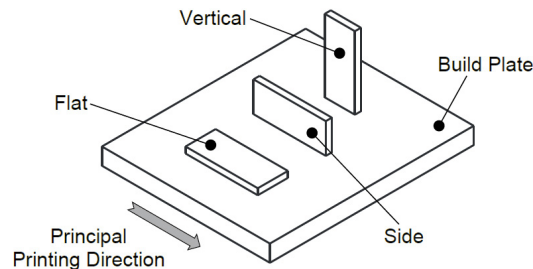


Fig. 2. Illustration of manufacturing direction on build plate.

For plain specimens,  $\theta_p$  was set at 0°, 30°, 45°, 60°, and 90°, whereas for notched specimens,  $\theta_p$  was set at 0°, 30°, and 45° (Ng and Susmel, 2020). The reason why notched specimens were only printed at the three specified angles is because the stress-strain behaviour of plain specimens with  $\theta_p$  equal to 30° and 45° was comparable to mechanical

properties of the specimens with  $\theta_p$  equal to  $60^\circ$  and  $90^\circ$  (Ng and Susmel, 2020). Fig. 6 (Ng and Susmel, 2020) which is shown later in the results section of this paper will serve as an evidence to the said observation. For C(T) specimens, the manufacturing parameters were set as recommended by ASTM D5045-14, with thickness of specimens varying in the range of 7 mm to 30 mm.

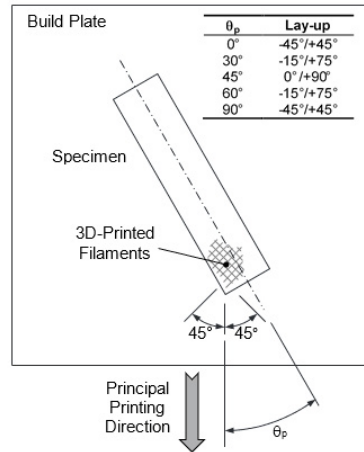


Fig. 3. Definition of the relationship between manufacturing angle,  $\theta_p$  and the corresponding material lay-up with respect to the manufacturing axis.

After completion of the manufacturing process, the specimens were then tested up to complete breakage by using the Shimadzu universal machine. The displacement rate was set to 2 mm/min, testing frequency set to 10 Hz and an extensometer with gauge length of 50 mm was employed during the tensile test for plain specimens (Ng and Susmel, 2020). The examples for the testing set-ups are shown in Fig. 4 (Ng and Susmel, 2020). The dog-bone plain specimens (Fig. 1a) and the specimens consisting two notches (Fig. 1c-e and Fig. 1i-l) were tested under tension, whereas the single notched specimens were loaded under three-point bending. The span between supports for specimens with single open notches (Fig. 1m-o) were set at 60 mm and the remaining single open notched specimens (Fig. 1f-h) were set equal to 50 mm (Ng and Susmel, 2020). A total of 128 samples were tested and post-processed to identify the mechanical properties of the AM ABS specimens.



Fig. 4. Examples of testing set-ups.

### 3. Results

The stress vs. strain curves obtained from tensile tests for plain specimens are shown in Fig. 5 (Ng and Susmel, 2020). It is worth noting that the stress-strain behaviour for all AM ABS plain specimens turns out to be linear up to the maximum stress. Therefore, clearly leading to the hypothesis that AM ABS materials can be modelled by linearising the stress-strain law until complete breakage (Ng and Susmel, 2020).

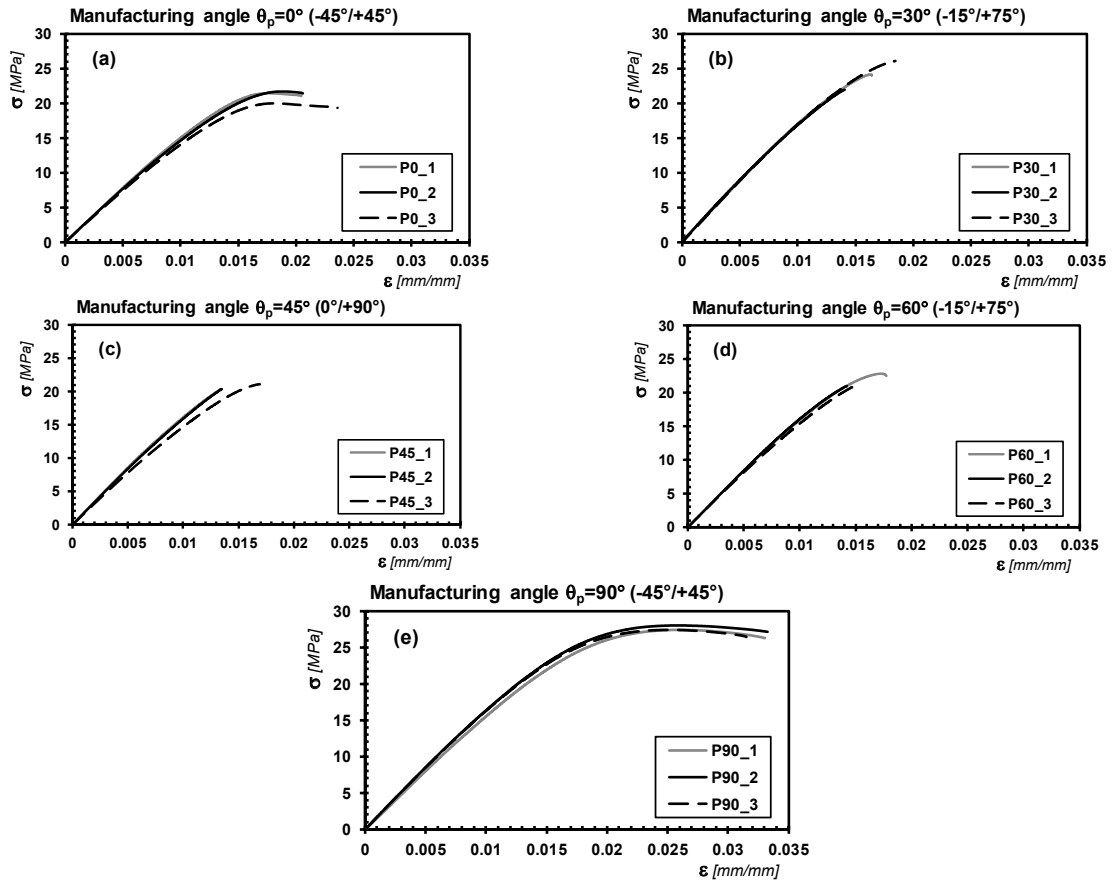


Fig. 5. Stress vs. strain curves obtained from tensile tests for plain specimens.

Besides that, the stress-strain curves for specimens manufactured at  $0^\circ$  and  $90^\circ$  (Fig. 5a and Fig. 5e) displayed the largest non-linear deformation, whereas specimens printed at  $30^\circ$ ,  $45^\circ$ , and  $60^\circ$  breaks as soon as maximum stress is reached (Ng and Susmel, 2020).

The mechanical properties that were post-processed from the stress-strain curves are: elastic modulus,  $E$ , 0.1% proof stress,  $\sigma_{0.1\%}$ , and ultimate tensile strength,  $\sigma_{UTS}$ . These mechanical properties are summarised in the charts of Fig. 6 (Ng and Susmel, 2020). From the charts shown in Fig. 6, it is evident that the mechanical response of the AM ABS specimens was affected by the manufacturing angle. However, from an engineering application point of view, the influence of manufacturing angle,  $\theta_p$  or material lay-up on the mechanical properties of the specimens is negligible as the investigated mechanical properties were all within two standard deviation of the mean as illustrated in Fig. 6 (Ng and Susmel, 2020). The recorded mean values for the discussed mechanical properties of plain specimens are as follows:  $E = 1590$  MPa,  $\sigma_{0.1\%} = 20.8$  MPa, and  $\sigma_{UTS} = 23.0$  MPa.

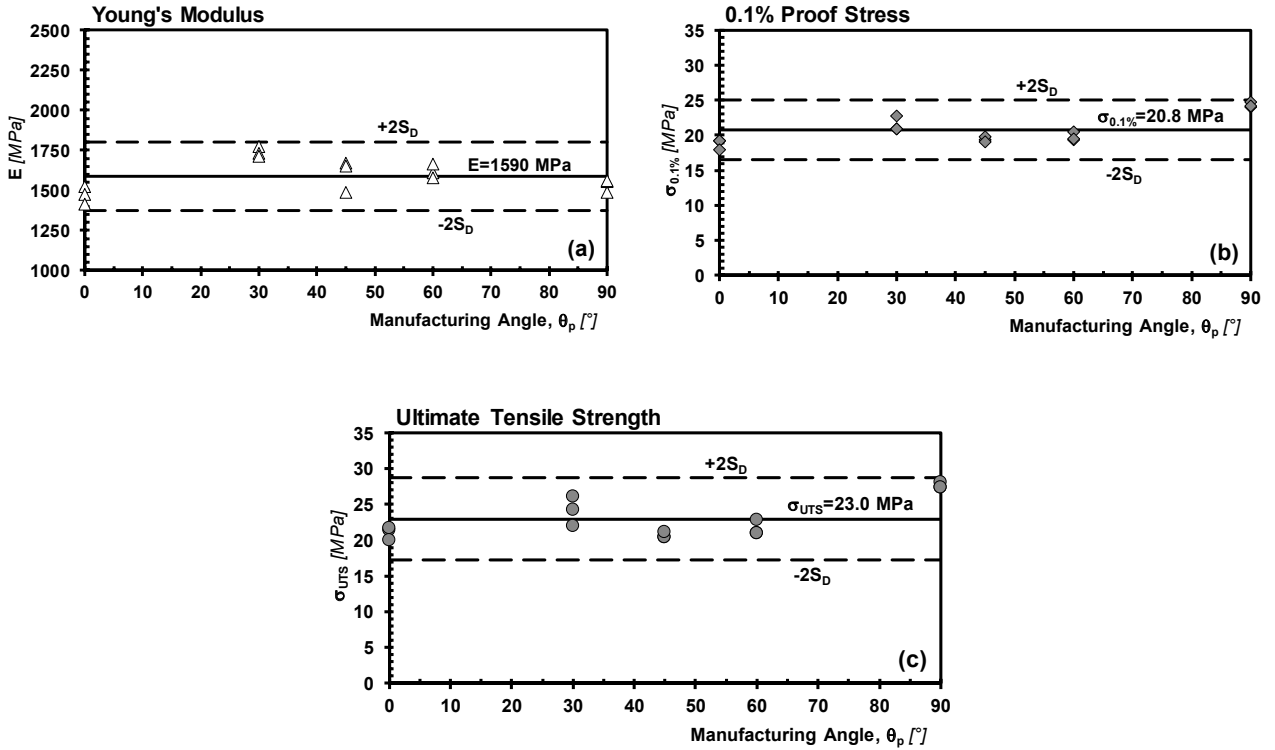


Fig. 6. Effect of manufacturing angle,  $\theta_p$  on Young's Modulus (a); 0.1% proof stress (b); and ultimate tensile strength (c).

For specimens in the presence of notches, an example of force vs. displacement curve for specimens loaded under tension is shown in Fig. 7a and an example of moment vs. deflection curve for specimens loaded under three-point bending is shown in Fig. 7b (Ng and Susmel, 2020).

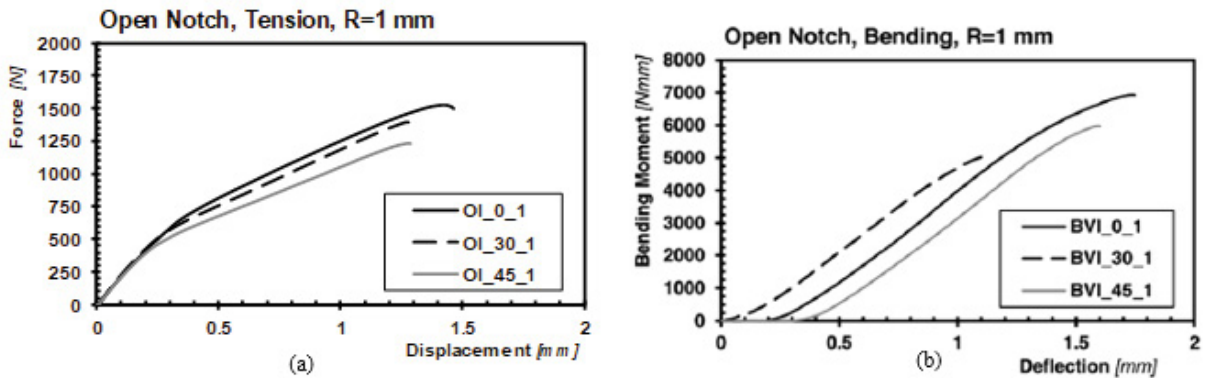


Fig. 7. Examples of mechanical response for notched specimens under tension (a) and bending (b).

Focusing on the results obtained from tensile testing, it is interesting to note that all force vs. displacement curves comprise of two linear branches, where the slope of the first linear branch is always steeper than the slope of the second linear branch irrespective of the notch sharpness and its notch opening angle,  $\alpha$  (Ng and Susmel, 2020). A plausible explanation to this phenomenon is that the difference in stiffness could be caused that the notched

specimens experienced two different failure mechanisms, where the initial deformation may be governed by the relative displacement between adjacent filaments and the subsequent deformation process may be mainly governed by the tensile properties of the individual filaments (Ng and Susmel, 2020). Clearly, further investigation has to be done to explain this interesting behaviour. As for the results obtained from three-point bending tests, an initial non-linear behaviour is always displayed in the moment vs. displacement curve. This behaviour is as expected as it is due to the mechanical adjustment of the rig at the start of the test (Ng and Susmel, 2020).

In terms of tensile testing of C(T) specimens, the plain strain fracture toughness,  $K_{IC}$  of the AM ABS specimens were computed as per the ASTM D5045-14 recommendations. The C(T) specimens were all manufactured at an angle of  $45^\circ$ , as it is the only manufacturing angle that results in a cracking behaviour that is governed by pure Mode I failure mechanism (Ng and Susmel, 2020). Further discussions related to the cracking behaviour of the AM ABS specimens will be addressed in the following cracking behaviour section of this paper. As a result, the average  $K_{IC}$  value was found to be equal to  $2.6 \text{ MPa}\cdot\text{m}^{1/2}$  under fully developed plain strain conditions (Ng and Susmel, 2020).

#### 4. Cracking behaviour

In order to investigate the influence of material lay-up on the cracking behaviour of the AM ABS specimens, both the crack initiation phase and crack propagation phase were observed and recorded accordingly. If attention is focused on the crack initiation phase, the crack paths for both notched and plain specimens always started on material planes almost perpendicular to the loading direction irrespective of the manufacturing angle,  $\theta_p$  (Ng and Susmel, 2020). Thus, suggesting the fact that the crack initiation phase for AM ABS specimens were dominated by the Mode I stress failure mechanism (Ng and Susmel, 2020). It is crucial to also note that the crack initiation process eventually results in a crack length that is approaching the shell thickness, which is 0.4 mm. Subsequently, the cracks were seen to propagate on zig-zag paths that are dependent on the material lay-up (Ng and Susmel, 2020).

In summary, the crack propagation phase of the plain and notched AM ABS specimens can be described by three failure mechanisms. The failure mechanisms are the debonding between adjacent filaments, debonding between adjacent layers, and the rectilinear cracking of extruded filaments (Ng and Susmel, 2020).

As mentioned in the previous section, the C(T) specimens were only manufactured at an angle of  $45^\circ$  with material lay-up of  $0^\circ/+90^\circ$ . Therefore, this results in a pure Mode-I failure mechanism during the crack propagation phase (Ng and Susmel, 2020). As for the crack initiation phase for the C(T) specimens, the cracks tended to grow slightly off the notch tip (Ng and Susmel, 2020). This occurrence could be due to the deposition method and material lay-up of the AM ABS material in the vicinity of the extremely sharp notch tip (Ng and Susmel, 2020).

#### 5. Application of the Theory of Critical Distances

Based on the results, the mechanical response shown by the tested AM ABS specimens leads to the two following simplifying hypotheses (Ng and Susmel, 2020):

- the AM ABS can be modelled as a homogenous and isotropic material;
- the mechanical behaviour of the tested AM ABS can be categorised as a linear-elastic and brittle material.

In this context, these two hypotheses are valid as long as the ABS components are additively manufactured flat on the build plate. Coincidentally, the hypotheses discussed above satisfy the condition for applying the Theory of Critical Distances (TCD) as a static assessment tool for the AM ABS engineering components (Taylor, 2007). Therefore, this paper also deals with the problem of validating the accuracy and robustness of TCD in assessing the static strength of the investigated AM ABS components.

In terms of the fundamentals of TCD, the static strength is estimated via an effective stress,  $\sigma_{\text{eff}}$  (Taylor, 2007). The value of  $\sigma_{\text{eff}}$  is derived based on the local linear-elastic stress field acting on component's notch tip region. It is assumed that the notched component will not break if the following condition is satisfied (Taylor, 2004; Taylor, Merlo, Pegley and Cavatorta, 2004; Susmel and Taylor, 2008):

$$\sigma_{eff} \leq \sigma_{UTS} \tag{1}$$

Note that the ultimate tensile strength,  $\sigma_{UTS}$  is obtained through the tensile tests of plain specimens (Taylor, 2004). On the other hand, the effective stress,  $\sigma_{eff}$  is computed via a critical distance,  $L$  which is a material length based on the microstructural heterogeneity. In order to calculate the critical distance,  $L$ , the following equation was adopted (Taylor, 2004; Whitney and Nuismer, 1974; Louks, Askes and Susmel, 2016):

$$L = \frac{1}{\pi} \left( \frac{K_{IC}}{\sigma_{UTS}} \right)^2 \tag{2}$$

Focusing on equation (2), the  $K_{IC}$  value is the plain strain fracture toughness and the critical distance,  $L$  is derived from two inherent material properties, which are  $K_{IC}$  and  $\sigma_{UTS}$ . This implies that the critical distance value is not affected by the notch profile and the notch sharpness (Taylor, 2007).

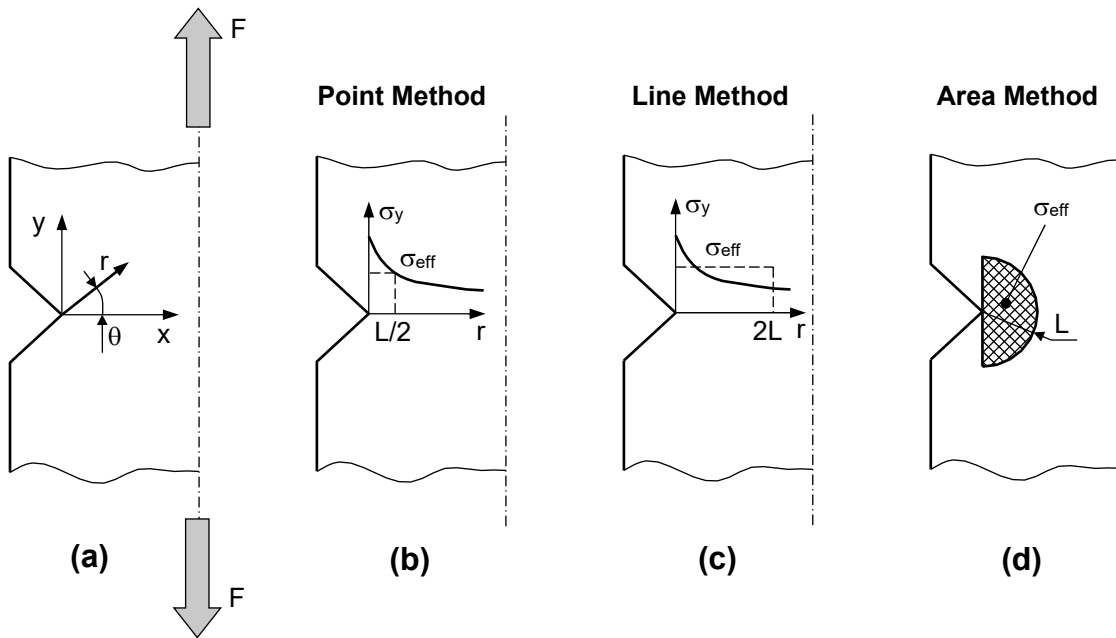


Fig. 8. Illustration of the formalisation Point Method (a); Line Method (b); and Area Method (c)

After determining the  $L$  value, the effective stress in terms of the TCD can be derived by adopting either of the three main methods. The methods are the Point, the Line, and the Area Method (Taylor, 2007). For the Point Method (PM), the  $\sigma_{eff}$  is defined to be equal to the local stress at a distance of  $L/2$  away from the notch tip as shown in Fig. 8b. The mathematical definition to obtain the  $\sigma_{eff}$  via the PM is as follows:

$$\sigma_{eff} = \sigma_y \left( \theta = 0^\circ, r = \frac{L}{2} \right) \tag{3}$$

As for the Line Method (LM), the  $\sigma_{eff}$  is determined by averaging the linear-elastic stress along the notch bisector over a distance of  $2L$  (Taylor, 2007; Taylor, 2004) as per Fig. 8c. The mathematical function that describes the relationship according to LM is as follows:

$$\sigma_{eff} = \frac{1}{2L} \int_0^{2L} \sigma_y(\theta = 0^\circ, r) \cdot dr \quad (4)$$

Finally, in terms of Area Method (AM), the  $\sigma_{eff}$  is calculated by averaging the linear-elastic stress over a semi-circle with its center being the notch tip which has a radius of  $L$  as depicted in Fig. 8d and is mathematically defined as follows (Taylor, 2007; Sheppard, 1991):

$$\sigma_{eff} = \frac{4}{\pi L^2} \int_0^{\frac{\pi}{2}} \int_0^L \sigma_1(\theta, r) \cdot r \cdot dr \cdot d\theta \quad (5)$$

In order to effectively apply the TCD as a static assessment tool for the AM ABS components, the local linear-elastic stresses in the vicinity of the notch tip were computed by using the commercial Finite Element (FE) code ANSYS® (Ng and Susmel, 2020).

As a result, the critical distance  $L$  is equal to 4.1 mm, which was calculated according to equation (2) by substituting the relevant values of material properties ( $\sigma_{UTS} = 23$  MPa and  $K_{IC} = 2.6$  MPa·m<sup>1/2</sup>) (Ng and Susmel, 2020). With regards to the method to obtain the effective stress,  $\sigma_{eff}$ , only the PM and AM were applied as this is due to the fact that the required integration limit  $2L$  when applying the LM, which is equal to 8.2 mm turns out to exceed half net-width of the tested specimens (Taylor, 2007).

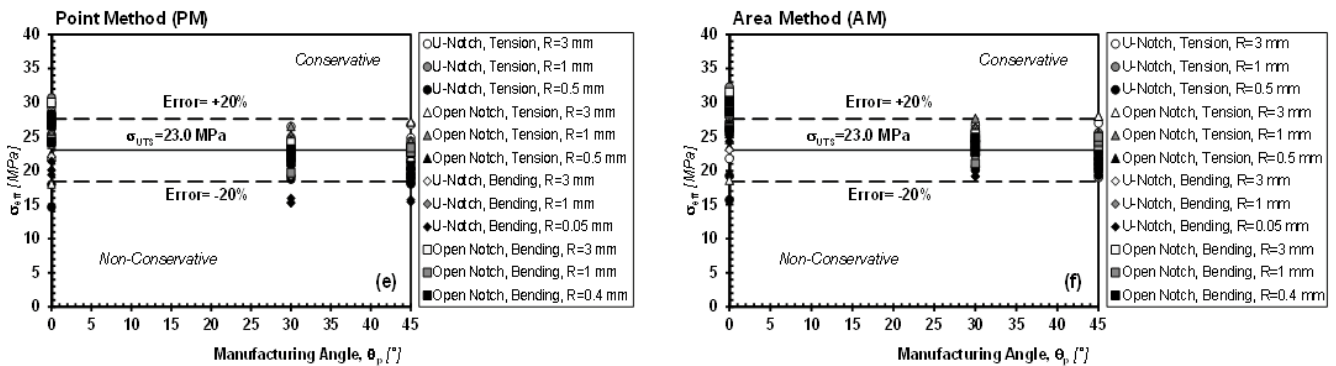


Fig. 9. Accuracy of the TCD in estimating the static strength of investigated specimens.

The resultant  $\sigma_{eff}$  values were then assessed accordingly to determine the accuracy of the TCD in estimating the static strength of the investigated AM ABS notched components. The error margin was calculated by using the formula as shown:

$$Error = \frac{\sigma_{eff} - \sigma_{UTS}}{\sigma_{UTS}} [\%]$$

This mathematical definition implies that a positive error value signifies a conservative estimate, whereas a negative error value represents a non-conservative estimate. The resulting accuracy of the static strength estimates by applying the TCD which is summarised in Fig. 9 is certainly rewarding as the estimates mainly fall within an error margin of  $\pm 20\%$  and signifies that it is applicable in engineering practice (Ng and Susmel, 2020).

## 6. Conclusions

The hypotheses for this investigation was successfully validated by testing a large number of AM ABS specimens in the presence of notches with various notch profiles and by analysing the experimental data via FE codes. In conclusion, the key findings from this investigation are as follows (Ng and Susmel, 2020):

- without the stress concentration effect, the mechanical properties of the AM ABS components can be assumed to be linear until final breakage occurs regardless of the material lay-up or the manufacturing angle,  $\theta_p$ ;
- the influence of the manufacturing angle,  $\theta_p$  on the relevant mechanical properties ( $E$ ,  $\sigma_{0.1\%}$ , and  $\sigma_{UTS}$ ) are negligible from an engineering practicality perspective as all the values fall within two standard deviation of the mean;
- an increase in the notch sharpness does not always lead to a decrease in the static strength of tested AM ABS specimens as the investigated material has a low notch sensitivity;
- the profile of the crack paths during crack propagation phase fully depends on the material lay-up;
- the TCD is proven to be a valid and accurate static assessment tool for the AM ABS engineering components as its estimates mainly fall within an error interval of  $\pm 20\%$ .

## Acknowledgements

The support for this work provided by the Faculty of Engineering of the University of Sheffield, Sheffield, UK and the funding of SURE scheme scholarship is deeply appreciated.

## References

- ASTM D5045-14, 2014. Standard Test Methods for Plane-Strain Fracture Toughness and Strain Energy Release Rate of Plastic Materials, ASTM International, West Conshohocken, PA, [www.astm.org](http://www.astm.org).
- Louks, R., Askes, H. and Susmel, L., 2016. A generalised approach to rapid finite element design of notched materials against static loading using the Theory of Critical Distances. *Materials & Design*, 108, pp.769-779.
- Ng, C. and Susmel, L., 2020. Notch static strength of additively manufactured acrylonitrile butadiene styrene (ABS). *Additive Manufacturing*, 34, p.101212.
- Sheppard, S., 1991. Field Effects in Fatigue Crack Initiation: Long Life Fatigue Strength. *Journal of Mechanical Design*, 113(2), pp.188-194.
- Susmel, L. and Taylor, D., 2008. The theory of critical distances to predict static strength of notched brittle components subjected to mixed-mode loading. *Engineering Fracture Mechanics*, 75(3-4), pp.534-550.
- Taylor, D., 2007. The theory of critical distances: a new perspective in fracture mechanics, Elsevier Ltd, Oxford, UK.
- Taylor, D., 2004. Predicting the fracture strength of ceramic materials using the theory of critical distances. *Engineering Fracture Mechanics*, 71(16-17), pp.2407-2416.
- Taylor, D., Merlo, M., Pegley, R. and Cavatorta, M., 2004. The effect of stress concentrations on the fracture strength of polymethylmethacrylate. *Materials Science and Engineering: A*, 382(1-2), pp.288-294.
- Whitney, J. and Nuismer, R., 1974. Stress Fracture Criteria for Laminated Composites Containing Stress Concentrations. *Journal of Composite Materials*, 8(3), pp.253-265.